OUT-OF-PLANE REATION OF RC STRUCTURAL WALLS IN NON-PRINCIPAL BENDING DIRECTIONS

ZHONGWEN. ZHANG [1*], and BING LI [2†]

[1]*Sch. of Civil & Env Eng., Nanyang Technological University, Singapore*
[2]*Sch. of Civil & Env Eng., Nanyang Technological University, Singapore*

ABSTRACT

Compared to column section, RC structural wall section often has much larger dimensions. Consequently, when loading direction of the wall is not parallel to its principal bending axes, large out-of-plane reaction may occur. However, very limited data is currently available regarding out-of-plane reaction and behaviour of RC walls.

This paper investigates the out-of-plane reaction in RC structural walls. Finite element (FE) analysis regarding an L-shaped wall in the experimental program in Nanyang Technological University is performed. Different aspects regarding the influence of out-of-plane reaction on performance of the wall are discussed. At last, an analytical solution based on Timoshenko beam theory is given regarding influence of out-of-plane reaction on curvature of the wall.

Keywords: Out-of-plane reaction; RC structural wall; multiple loading directions; Timoshenko beam theory; curvature; finite element analysis.

1. INTRODUCTION

Structural RC walls are commonly used in medium-rise or high-rise buildings due to their large in-plane and out-of-plane stiffness. Often in accordance to the architectural plan, the principal bending axes of these walls cannot be placed parallel to the principal directions of the building. Also, as earthquake attack often imposes lateral loads in both principal directions of the building, structural walls are expected to resist lateral loads in non-principal bending directions frequently.(Paulay and Priestley 1992)

Elastic bending theory states that for a section resisting bending moments not parallel to its principal axes (which are the axis of symmetry and the direction perpendicular to the axis for a symmetrical section), the neutral axis of the section is not parallel to its bending moment. Instead, an angle exists as(Boresi and Schmidt 2002):

[*] Presenter: Email: chuangwendell@gmail.com

[†] Corresponding author: Email: CBLI @ntu.edu.sg

$$\tan\alpha = \frac{I_z}{I_y}\tan\theta \tag{1}$$

in which, α is given as the inclination of the neutral axis while θ is the angle between the moment and the principal bending axes, I_z and I_y are moment of inertia in principal bending direction Z and Y, as Figure 1 shows.

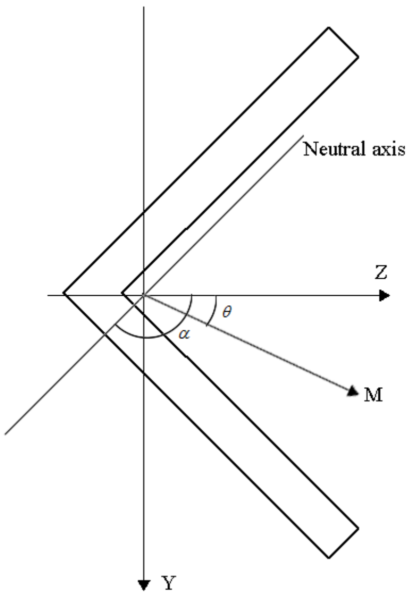

Figure 1: Pure bending of an unsymmetrical section.

In designing of structural wall systems, engineers assume that lateral displacements of individual structural walls are compatible at floor levels as the floor diaphragms can transfer in-plane force.(Paulay and Priestley 1992) Consequently, a bending moment perpendicular to the top displacement is expected for a structural wall when neither its principal bending axis coincides with roof displacement of the building. In this paper, the directions parallel to top displacement of the wall are referred as in-plane directions. As top displacement of the wall will introduce moment and shear force in the plane perpendicular to the top displacement, these reactions are referred as out-of-plane reactions.

2. OUT-OF-PLANE REACTION AND ITS INFLUENCE ON BEHAVIOUR OF THE WALL

2.1. Out-of-plane reaction in tested L-shaped RC wall

An experimental program regarding seismic performance of non-rectangular RC walls is conducting in Nanyang Technological University which includes tests on L-shaped and T-shaped RC walls with different configurations. In several cases, the lateral loads were applied parallel to one of the wall segments of the tested L-shaped wall, which were in 45 degrees with the principal bending axes of the wall. Details regarding the test program are provided in Figure 2.

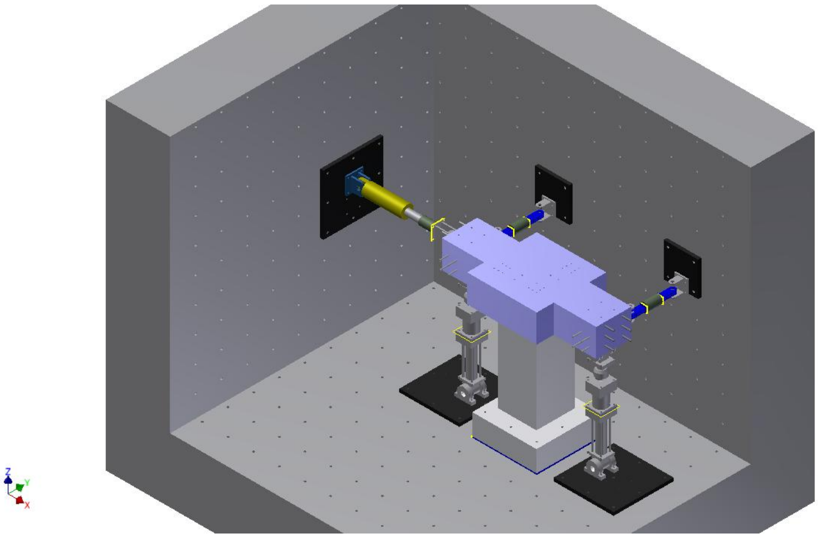

Figure 2: An example of figure style.

Based on the L-shaped wall in the experimental program, FE analysis was carried out to provide more information regarding performance of the wall. The analysis predicted load-deformation loops are shown in Figure 3.

Figure 3b shows predicted out-of-plane reaction for the L-shaped RC wall. In general, maximum out-of-plane reaction for L-shaped RC wall was approximately half of the maximum in-plane reaction. However, as Figure 4 shows, the ratio between out-of-plane reaction and in-plane reaction was not constant. The out-of-plane resistant can be much larger than the in-plane resistant. This phenomenon mainly happened in the unloading processes.

2.2. Influence of out-of-plane reaction in flexural behaviour of RC structural wall

Also, as shown in Figure 5, curvature in the out-of-plane direction was observed in the wall even though displacement in out-of-plane direction was restrained at top of the wall. This phenomenon may come from the geometrical compatibility between wall shear and flexural deformations. When the wall is not loaded parallel to its principal bending directions, shear deflection parallel to flange of the wall exists due to out-of-plane reaction. As out-of-plane displacement is restrained in bottom and top of the wall, out-of-plane curvature is imposed to the wall. Detailed discussions regarding this issue can be found in Section 3.2.

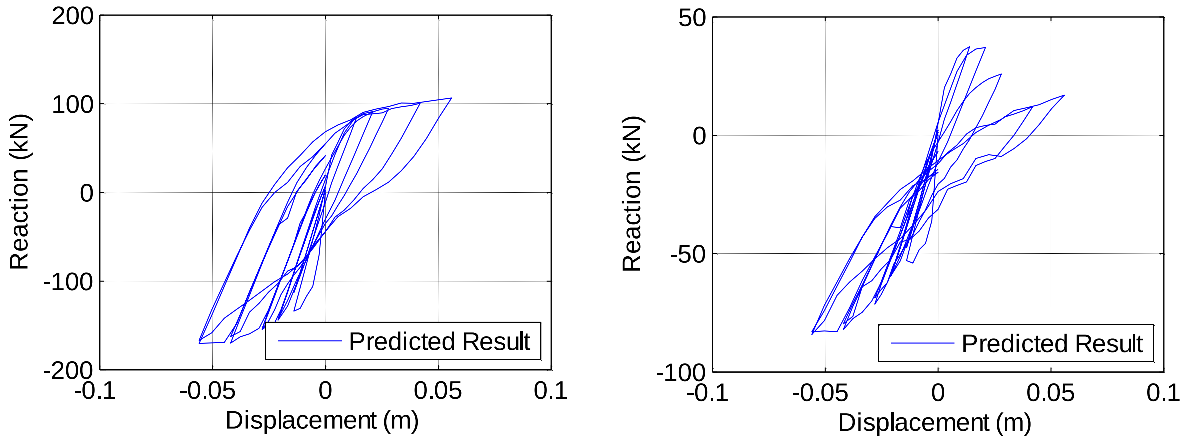

(a) In-plane (b) Out-of-plan

Figure 3: Deformation-reaction hysteresis loops for in-plane and out-of-plane.

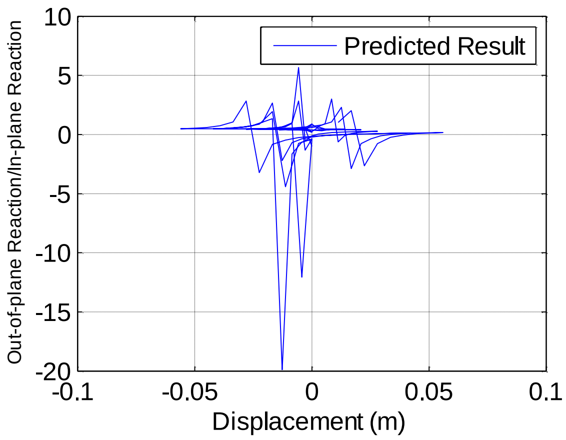

Figure 4: Ratio of in-plane and out-of-plane direction lateral reaction force.

2.3. Influence of out-of-plane reaction in shear behaviour of RC structural wall

In addition to the flexural behaviour, the out-of-plane reaction has influenced shear behaviour of the wall. Figure 6 shows the FEM predicted in-plane and out-of-plane reaction forces at base of the wall in different lateral drift ratios. It can be found that a large component of the out-of-plane reaction force is carried by the tip of the web at a high lateral drift ratio. This is understandable as at a high lateral drift ratio, shear stiffness of the section reduces due to tension cracks. Table 1 lists the portion of shear force carried by individual wall segments at different lateral drift ratios. At a lateral drift ratio of 1%, the web almost carries half of the out-of-plane reaction.

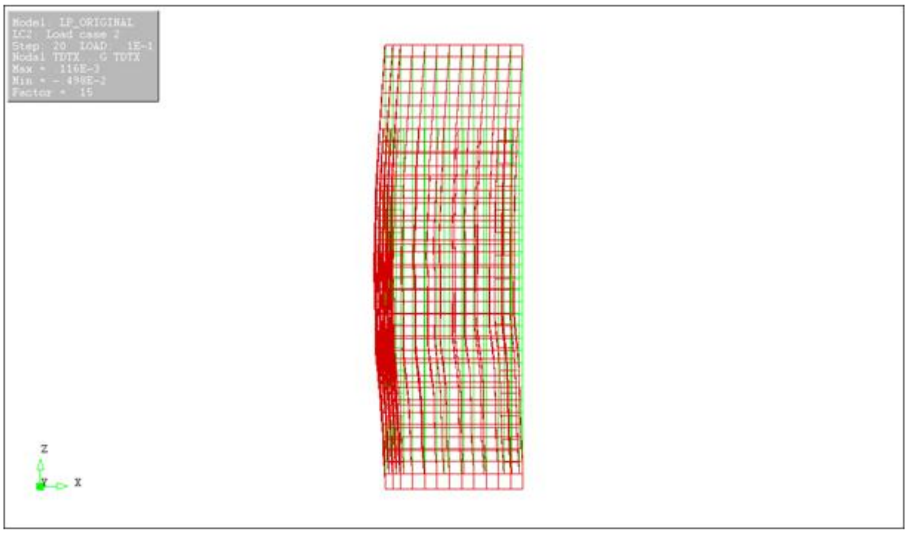

Figure 5: Deflection of the wall in out-of-plane direction.

Table 1: Portion of shear force carried by flange and web of the wall

Drift ratio 0.25%				Drift ratio 1.0%			
Out-of-plane		In-plane		Out-of-plane		In-plane	
Web	Flange	Web	Flange	Web	Flange	Web	Flange
7.4%	92.5%	89.9%	10.1%	40.0%	60.0%	99.0%	1%

3. ANALYTICAL SOLUTION ON OUT-OF-PLANE REACTION AND ITS INFLUENCE USING ELASTIC TIMOSHENKO BEAM THEORY

Analytical solutions are presented in this section using Timoshenko beam theory regarding out-of-plane reaction and its influence on curvature of the wall. The predicted results are compared with the FE analytical data to estimate their accuracy. At last, a parametric study regarding influence of out-of-plane reaction on curvature of the wall is conducted using the proposed solutions.

3.1. Out-of-plane reaction

Using the elastic bending theory, the out-of-plane reaction for L-shaped wall can be easily calculated from the area moments of inertia of the section in the two principal loading directions as shown in Equation 1.

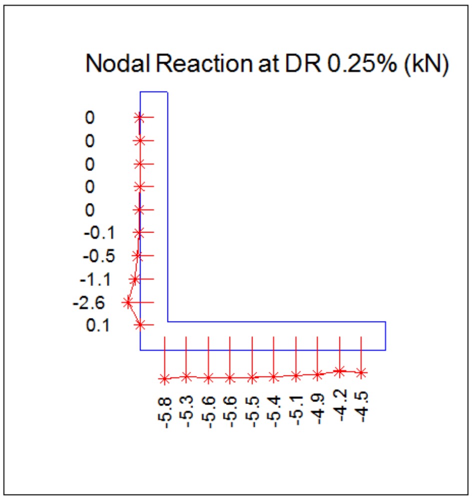

(a)

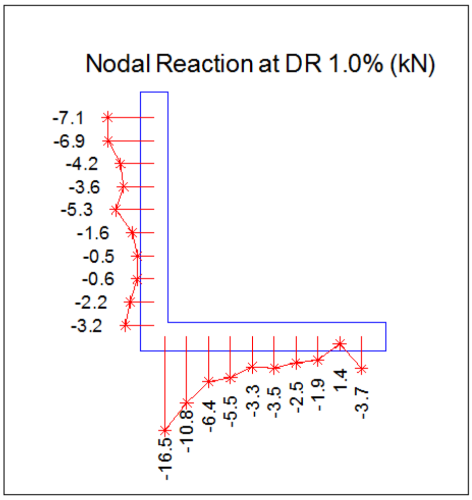

(b)

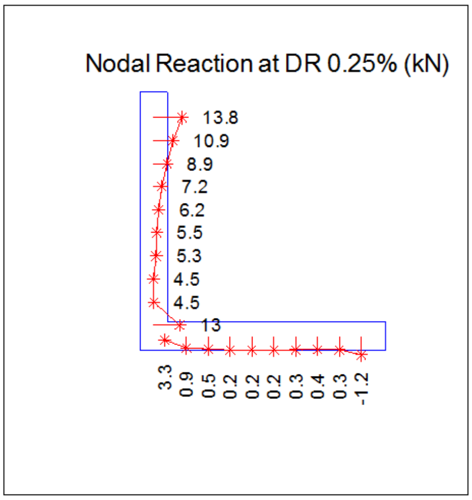

(c)

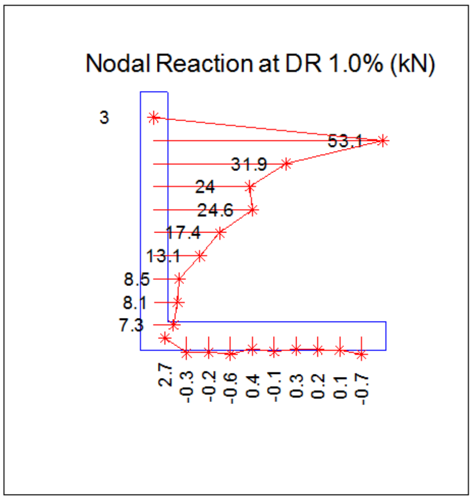

(d)

Figure 6: Numerically determined distribution of reaction forces at the base of the wall (a) out-of-plane force (b) out-of-plane force (c) in-plane force (d) in-plane force.

Therefore, when the loading direction of the wall is parallel to the wall web, the ratio of in-plane moment reaction to the out-of-plane moment reaction is approximately 1.83. This prediction is compared with the FE predicted pushover result in Figure 7. It seemed that for the L-shaped wall the elastic bending theory generally predicted reliable results for the out-of-plane bending moment with some conservation. However, as the wall experienced more inelastic deformation, the ratio varied from the calculated result.

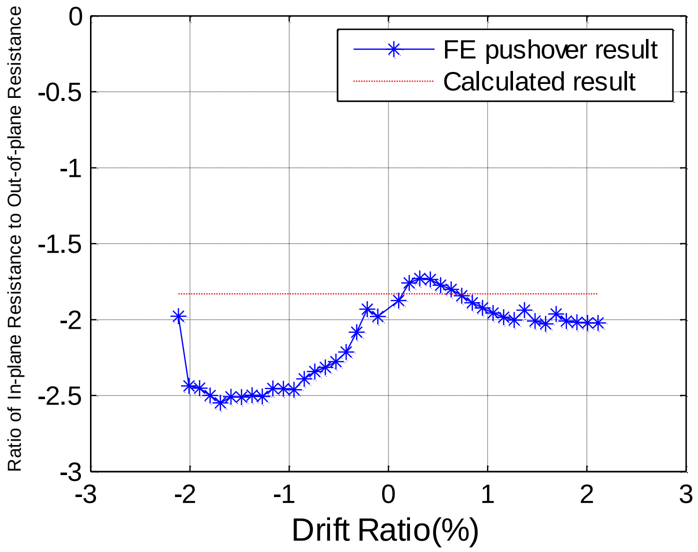

Figure 7: Comparison of the calculated result and the FE pushover result.

3.2. Influence of out-of-plane reaction on curvature of the wall

As Section 2.2 shows, the FE analytical results demonstrate that curvature of the wall is influenced by the out-of-plane reaction. An curvature in out-of-plane direction is imposed on the wall. This phenomenon can be critical sometimes as out-of-plane curvature can impose additional compression strain to the wall section. A solution for predicting influence of out-of-plane reaction on curvature of the wall is proposed in this section using elastic Timoshenko beam theory.

3.2.1. Analysis on curvature of the wall using Timoshenko beam theory

As Figure 5 shows, the out-of-plane curvature was introduced to the wall section for the L-shaped wall. An analytical solution based on elastic Timoshenko beam theory is given as follows.

Considering the elastic behaviour of the wall, the wall is restrained only at the base and top section. Therefore, the deformation shape of the wall can be assumed as:(Gere and Timoshenko 1984)

$$u = a_0 + a_1 x + a_2 x^2 + a_3 x^3$$

$$v = b_0 + b_1 x + b_2 x^2 + b_3 x^3 \qquad (2)$$

To avoid coupling of wall deflections in different directions, the u and v axis are set parallel with the principal axes of the wall section as shown in Figure 8.

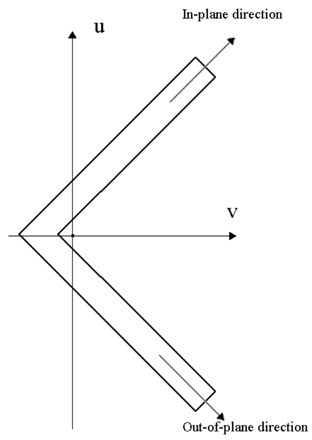

Figure 8: Coordinate system for the analysis.

The wall is fully restrained at the bottom. At top of the wall, the in-plane direction is free-end. Displacement in out-of-plane direction is restrained at top of the wall. Rotation in out-of-plane direction at top of the wall is assumed to be unrestrained.

Assuming top-displacement of wall in the in-plane direction is Δ, the boundary conditions can be written as:

1. Fixed end at wall base;

(a) $u(0) = 0$ (b) $v(0) = 0$

(c) $\Theta_u(0) = 0$ (d) $\Theta_v(0) = 0$

2. Out-of-plane displacement restrained and free rotation at both in-plane and out-of-plane directions;

(e) $\sqrt{2}/2*\left[u(l) - v(l)\right] = 0$ (f) $\sqrt{2}/2*\left[u(l) + v(l)\right] = \Delta$

(g) $M_{Inplane}(l) = EI_{Inplane}\dfrac{\partial\Theta_{Inplane}(l)}{\partial x} = 0$ (h) $M_{Outplane}(l) = EI_{Outplane}\dfrac{\partial\Theta_{Outplane}(l)}{\partial x} = 0$

In which Θ is the angle due to pure bending. For a Timoshenko beam,

$$\Theta(x) = \frac{dw}{dx} - \frac{V(x)}{\kappa^2 GA}$$

By replacing Θ in equation c, d, g and h, these equations can be rewritten as:

(c) $\left.\dfrac{du}{dx}\right|_{x=0} - \dfrac{V_u}{\kappa_v{}^2 GA} = 0$ (d) $\left.\dfrac{dv}{dx}\right|_{x=0} - \dfrac{V_v}{\kappa_v{}^2 GA} = 0$

(g) $\left.\frac{d^2(u+v)}{dx^2}\right|_{x=l} - \frac{V_u^{'}(l)+V_v^{'}(l)}{\kappa^2 GA} = \left.\frac{d^2(u+v)}{dx^2}\right|_{x=l} = 0$

(h) $\left.\frac{d^2(u-v)}{dx^2}\right|_{x=l} - \frac{V_u^{'}(l)+V_v^{'}(l)}{\kappa^2 GA} = \left.\frac{d^2(u-v)}{dx^2}\right|_{x=l} = 0$

in which V_u and V_v can be written as a function of Δ:

$$\frac{\sqrt{2}}{2}\Delta = \left(\frac{l^3}{3EI_u} + \frac{l}{\kappa_u^{\,2} GA}\right)V_u$$

$$\frac{\sqrt{2}}{2}\Delta = \left(\frac{l^3}{3EI_v} + \frac{l}{\kappa_v^{\,2} GA}\right)V_v$$

Applying the boundary condition equations a to h to the wall shape function, eight equations can be derived for eight unknowns as shown in Equation 3.

For the out-of-plane direction, the deflection curve is given as:

$$w_{out-of-plane} = \sqrt{2}/2*(u-v) = \sqrt{2}/2*\left[(a_0-b_0)+(a_1-b_1)x+(a_2-b_2)x^2+(a_3-b_3)x^3\right]$$

Consequently, as Equation 3 indicates, for a given drift ratio, $w_{out-of-plane}$ is only influenced by $V_u l/\kappa_u GA$ and $V_v l/\kappa_v GA$ which are the elastic shear displacements Δ_{su} and Δ_{sv} at top of the wall in two principal bending directions. Figure 9a shows the predicted out-of-plane displacement using Equation 3 for the L-shaped wall at lateral drift ratio of 0.2 percent. The predicted result matched with the FE analysis result well. Figure 9b shows the calculated result of the wall at lateral drift ratio of 1 percent. In general, at lateral drift ratio of 1 percent the calculated result underestimated out-of-plane curvature of the L-shaped wall significantly. This is understandable as the calculation used the elastic shear stiffness which may underestimate shear deformation of the wall significantly as indicated by Beyer et al. (Beyer, Dazio et al. 2008).

As Equation 2 generally applies to deflection shape of the wall until large plastic hinge occurs in the wall. As long as the correct Δ_{su}/Δ_u (shear deformation over total deformation in u direction at wall top) and Δ_{su}/Δ_{sv} (shear deformation in u direction over shear deformation in v direction at wall top) ratios are given, the calculated result should be able to approximate the out-of-plane curvature for the L-shaped wall in the experimental program. It is observed by Beyer et al. (Beyer, Dazio et al. 2008) that the ratio of shear deformation to flexural deformation for individual wall segment remains approximately constant. Based on this observation, Δ_{su}/Δ_u is assumed as 0.2 which is similar to ratio of shear deformation to total deformation in the U-shaped wall tested by Beyer et al.

(Beyer, Dazio et al. 2008) with a shear span ratio of 2.81. Also assumed is that Δ_{su}/Δ_{sv} remains the same. Figure 9b also shows the calculated result from the modified Δ_{su}/Δ_{u} ratio. The calculated result with modified Δ_{su}/Δ_{u} agrees with the FE analysis data. However, distribution of curvature in the wall is more complex than the calculated result as bending stiffness of the wall section varies when the wall reaches nonlinear stage.

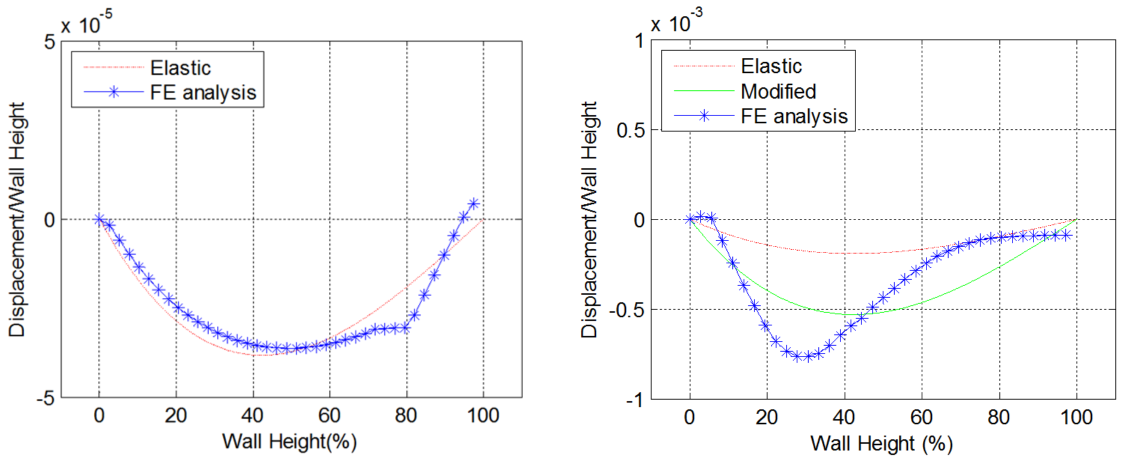

(a) (b)

Figure 9: Comparison of the calculated and FE analytical out-of-plane deflection of L-shaped wall at (a) lateral drift ratio 0.2% (b) lateral drift ratio 1.0%.

$$\begin{bmatrix} 1 & 0 & 0 & 0 & 0 & 0 & 0 & 0 \\ 0 & 1 & 1 & 1 & 0 & 0 & 0 & 0 \\ 0 & 1 & 0 & 0 & 0 & 0 & 0 & 0 \\ 0 & 0 & 1 & 3 & 0 & 0 & 1 & 3 \\ 0 & 0 & 0 & 0 & 1 & 0 & 0 & 0 \\ 0 & 0 & 0 & 0 & 0 & 1 & 1 & 1 \\ 0 & 0 & 0 & 0 & 0 & 1 & 0 & 0 \\ 0 & 0 & 1 & 3 & 0 & 0 & -1 & -3 \end{bmatrix} \begin{bmatrix} a_0 \\ a_1 l \\ a_2 l^2 \\ a_3 l^3 \\ b_0 \\ b_1 l \\ b_2 l^2 \\ b_3 l^3 \end{bmatrix} = \begin{bmatrix} 0 \\ \frac{\sqrt{2}\Delta}{2} \\ \frac{V_u l}{\kappa_u{}^2 GA} \\ 0 \\ 0 \\ \frac{\sqrt{2}\Delta}{2} \\ \frac{V_v l}{\kappa_v{}^2 GA} \\ 0 \end{bmatrix} \tag{3}$$

3.2.2. Influence of shear deformation on curvature of the wall

As indicated in Section 3.2.1, curvature of the wall is influenced by the ratio of shear deformation to total deformation Δ_{su}/Δ_{u} and the ratio of shear deformation in different directions Δ_{su}/Δ_{sv}. To further investigate this influence, using the solution presented in Section 3.2.1, a parametric study is conducted regarding the influence of different Δ_{su}/Δ_{u} and Δ_{su}/Δ_{sv} ratios. The ratios of

Δ_{su}/Δ_u investigated range from 0.05 to 0.3. The ratios of Δ_{su}/Δ_{sv} investigated range from 1.0 to 5.5. The in-plane lateral drift ratio set for these calculations is 1 percent. Figure 10 shows the calculated deflection curves for these ratios. As the top of the wall is restrained from displacement in out-of-plane direction, maximum displacement occurs approximately at mid span. The deflection in out-of-plane direction increases as the ratio of Δ_{su}/Δ_u or Δ_{su}/Δ_{sv} increases. The maximum deflection in the out-of-plane direction for the investigated cases is around 0.08 percent of the wall height.

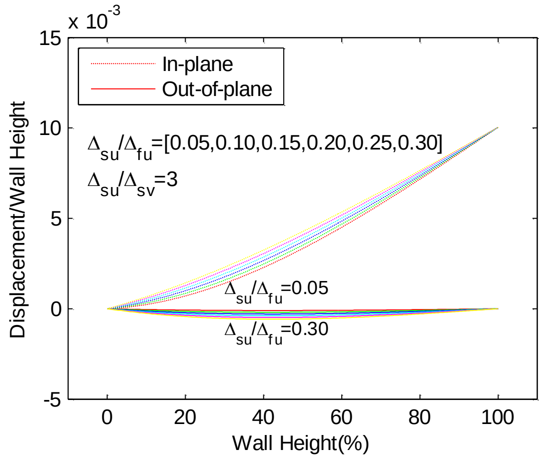

(a)

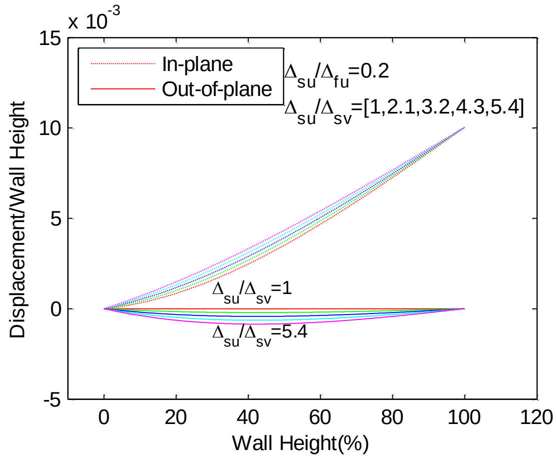

(b)

Figure 10: Calculated deflection curve for different Δ_{su}/Δ_u and Δ_{su}/Δ_{sv} ratios for in-plane and out-of-plane direction

Figure 11 shows that the calculated curvature of deflection curves in Figure 10. The out-of-plane curvature, as the deflection, increased with Δ_{su}/Δ_{sv} or Δ_{su}/Δ_{sv} . Specifically, there was no curvature of the wall in out-of-plane direction when Δ_{su}/Δ_{sv} equaled 1. Also, as the out-of-plane curvature increased, the in-plane curvature of the wall decreased. When Δ_{su}/Δ_u equaled 0.3 and Δ_{su}/Δ_{sv} equaled 3, the maximum in-plane curvature of the wall decreased by 60.8% while the out-of-plane curvature was 65.4% of the in-plane curvature. On the other hand, for the case with Δ_{su}/Δ_u equaled 0.2 and Δ_{su}/Δ_{sv} equaled 5.5, the out-of-plane curvature can be larger than the in-plane curvature. By maximum, curvature of the wall can be reduced by reduced by 60.8% for the parameters investigated.

As the ratios of Δ_{su}/Δ_{sv} investigated in this paper are believed to be common for L-shaped RC structural walls, the influence of out-of-plane reaction on curvature of the wall in both in-plane and out-plane directions can be quite significant. Further investigation regarding this issue is needed.

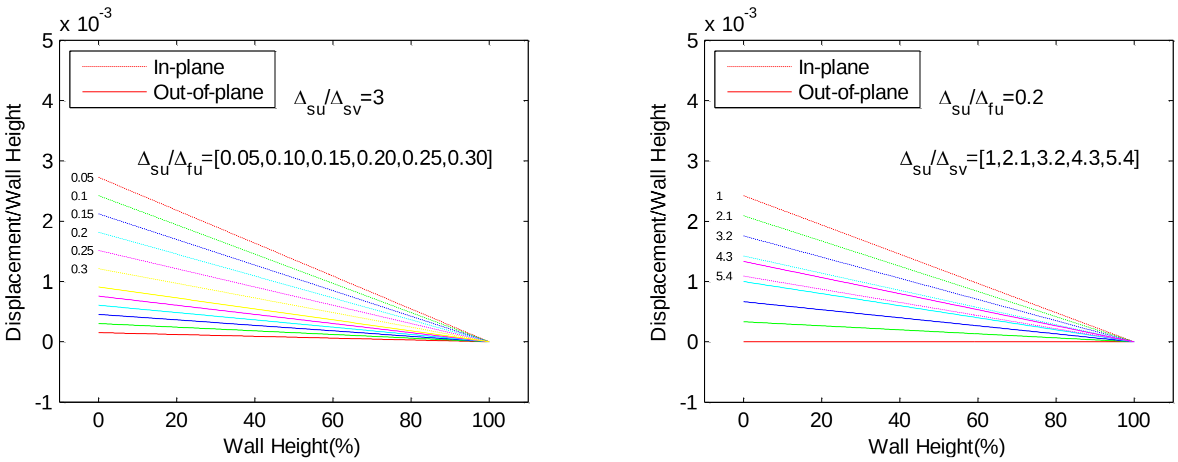

(a) (b)

Figure 11: Calculated yield curvature for different Δ_{su}/Δ_{u} and Δ_{su}/Δ_{sv} ratios for in-plane and out-of-plane direction.

4. CONCLUSIONS

Out-of-plane reactions are introduced to a section when its loading direction is not parallel to its principal bending axes. In this paper, FE analysis is carried out regarding out-of-plane behaviour of an L-shaped RC wall tested in Nanyang Technological University. The magnitude and influences of the out-of-plane reaction are presented. At last, a solution based on Timoshenko beam theory is given regarding influence of out-of-plane reaction on curvature of the wall. The main conclusions drawn from the study are:

1. When a wall is not loaded parallel to the principal bending axes of its section, an out-of-plane reaction exists. For the L-shaped RC structural wall, maximum out-of-plane reaction force is approximately 48.4% of the maximum in-plane reaction force.

2. Shear force in out-of-plane direction is introduced to the wall due to the reaction. At high lateral drift ratio, a large portion of the out-of-plane shear force is carried by the wall web.

3. The elastic bending theory in general predicts out-of-plane reaction of the tested wall well. However, the prediction may not apply to unloading branch of the hysteresis loops.

4. An analytical solution based on Timoshenko beam theory is given regarding out-of-plane curvature of the wall. Comparison with FE analysis data shows that the solution is accurate in elastic range. In inelastic range, modifying Δ_{su}/Δ_{u} ratio assumed in the solution gives better prediction.

5. The solution shows that as the curvature in out-of-plane direction increases, curvature of the wall in in-plane direction decreases. For investigated Δ_{su}/Δ_{u} and Δ_{su}/Δ_{sv} ratio, the

in-plane curvature of the wall can decrease by 60.8%. On the other hand, the out-of-plane curvature of the wall can be larger than the in-plane curvature. Further investigation is needed regarding this issue.

REFERENCES

Beyer, K., et al. (2008). Elastic and inelastic wide-column models for RC non-rectangular walls. 14th World Conference on Earthquake Engineering. Beijing, China.

Beyer, K., et al. (2008). "Quasi-static cyclic tests of two U-shaped reinforced concrete walls." Journal of Earthquake Engineering 12(7): 1023-1053.

Boresi, A. P. and Schmidt, R. J. (2002). Advanced Mechanics of Materials. New York, John Wiley & Sons, Inc.

Gere, J. M. and Timoshenko, S. (1984). Mechanics of materials. Monterey, Calif., Brooks/Cole Engineering Division.

Paulay, T. and Priestley, M. J. N. (1992). Seismic Design of Reinforced Concrete and Masonry Buildings, John Wiley & Sons, Inc.